Metallic ferromagnetism in a single-band model. II. Finite-temperature magnetic properties

J. E. Hirsch
Department of Physics, B-019, University of California–San Diego, La Jolla, California 92093
(Received 20 June 1989)

A recently proposed band model to describe metallic ferromagnetism is studied at finite temperatures within the mean-field approximation. We discuss in particular the behavior of critical temperature, specific heat, magnetic susceptibility above T_c, and magnetization below T_c assuming a constant density of states. The model overcomes in a simple way the major difficulties of Stoner theory and yields properties that are consistent with a variety of observations in ferromagnetic metals and alloys.

I. INTRODUCTION

A great deal about the physics of a phenomenon can be learned by identifying the simplest possible model that contains its essential features. In a recent paper[1] (hereafter referred to as I) we have proposed what we believe to be such a model to describe metallic ferromagnetism. The Hamiltonian is given by

$$H=-t\sum_{\substack{\langle ij\rangle\\ \sigma}}(c_{i\sigma}^{\dagger}c_{j\sigma}+\text{H.c.})+U\sum_{i}n_{i\uparrow}n_{i\downarrow}+J\sum_{\substack{\langle ij\rangle\\ \sigma\sigma'}}c_{i\sigma}^{\dagger}c_{j\sigma'}^{\dagger}c_{i\sigma'}c_{j\sigma}\ , \tag{1}$$

describing tight-binding electrons in a single band. The parameter J is an off-diagonal matrix element of the Coulomb interaction between electrons in Wannier states ϕ_i at nearest-neighbor sites:

$$J=\int d^3r\,d^3r'\phi_i^*(r)\phi_j^*(r')\frac{e^2}{|r-r'|}\phi_i(r')\phi_j(r) \tag{2}$$

and is positive, and U is the usual Hubbard on-site repulsion.[2] Although U is much larger than J we have proposed that the term containing J is the *relevant* operator for metallic ferromagnetism and thus cannot be omitted. It was shown in I that the Hamiltonian Eq. (1) naturally describes situations with full-spin polarization (strong ferromagnets) and partial-spin polarization (weak ferromagnets), independent of details of the density of states. In this paper we examine the properties of the Hamiltonian Eq. (1) at finite temperatures.

The field of metallic ferromagnetism has a long history (see, for example, Refs. 3 and 4 and references therein) that is characterized by a "dichotomy" between band and localized pictures.[5] In particular, it is often stated that the band model naturally describes certain features of the problem (nonintegral number of Bohr magnetons, transport properties, etc.) and the localized model others (Curie-like susceptibility, temperature dependence of magnetization, magnitude of T_c, etc.). One way out of this dilemma has been to talk about coexisting localized and itinerant electrons,[6] which may provide a useful qualitative picture but is difficult to translate into a consistent mathematical theory. A second way out has been to incorporate spin-fluctuation corrections into the band model,[7] which leads to complicated theories that need to rely on uncontrolled approximations.

As metallic ferromagnets are metals, it is naturally preferable to describe them using band theory. This has been done within what is usually called Stoner theory,[8,9] where a featureless exchange energy is added to band electrons in a solid. The main drawback of Stoner theory in our opinion is that the properties of the model are determined by the detailed behavior of the density of states. For example, the theory predicts only zero- or full-spin polarization if the density of states is constant throughout the band,[10] and a narrow range of partial-spin polarization for a free-electron density of states.[11] Similarly, the magnitude of T_c and of the susceptibility above T_c are largely determined by the magnitude of the first and second derivatives of the density of states at the Fermi energy, and certain shapes of the density of states can drive the transition first order.[12] This situation is not very satisfying, as we do not know of any fundamental reasons that determine the fine structure of the density of states in a metal. In addition, the Stoner model has difficulty in describing weak ferromagnetism, Curie-Weiss susceptibility, shape of magnetization curves, and magnitude of specific-heat jumps even if the density of states is arbitrarily chosen.

In this paper we explore some features of the model Eq. (1) at finite temperatures within mean-field theory and show that our model overcomes several difficulties of the Stoner model. The results do not crucially depend on fine details of the density of states, and thus for most of the discussion we use a constant density of states throughout the band. Weak ferromagnetism, Curie-Weiss law above T_c, large specific-heat jumps, and some of the observed systematics of T_c and shape of magnetization curve versus band filling follow naturally from our simple treatment. Furthermore, the observed anomalous drop of resistivity below T_c in ferromagnetic metals[13] is a necessary consequence of our model.

In addition, our theory provides a new and intuitively appealing picture of metallic ferromagnetism. As the temperature is lowered, the electron-electron interaction described by the last term in Eq. (1) causes the bands to become increasingly narrow, thus raising the electronic energy and increasing the internal pressure. At the criti-

 ©1989 The American Physical Society

cal temperature it starts to become advantageous to spin polarize because this causes the split bands to widen again with increasing magnetization. It is as if the solid is "breathing in" below T_c, which also causes the anomalously large lattice constants and magnetoelastic effects observed in ferromagnetic metals.

The paper is organized as follows. In Sec. II we derive the relevant equations at finite temperatures and discuss qualitatively their properties. In the limit of T_c much less than the bandwidth most results can be obtained analytically within the Sommerfeld expansion, but it rapidly becomes inaccurate for higher temperatures. In Sec. III we discuss numerical results of the self-consistent equations for a variety of cases to illustrate the principal trends. We conclude in Sec. IV with a summary of results and a discussion.

II. THEORY

We obtain the mean-field equations describing ferromagnetism for the Hamiltonian Eq. (1) by allowing for a finite-expectation value of $\langle c^{\dagger}_{k\sigma} c_{k\sigma} \rangle$ which is different for $\sigma =$ up, down, and performing a mean-field decoupling of the interactions. The procedure is standard and is discussed in I for our case. The resulting self-consistent equations are

$$m = \int_{-D/2}^{D/2} d\varepsilon\, g(\varepsilon)[f(E_+(\varepsilon)) - f(E_-(\varepsilon))] , \tag{3a}$$

$$n = \int_{-D/2}^{D/2} d\varepsilon\, g(\varepsilon)[f(E_+(\varepsilon)) + f(E_-(\varepsilon))] , \tag{3b}$$

$$E_\sigma(\varepsilon) = \left[1 - \frac{2JzI_1}{D}\right]\varepsilon - \sigma\left[\frac{U+Jz}{2} + H\right]m - \mu , \tag{4}$$

$$I_1 = \int_{-D/2}^{D/2} d\varepsilon\, g(\varepsilon)\left[-\frac{\varepsilon}{D/2}\right][f(E_+(\varepsilon)) + f(E_-(\varepsilon))] . \tag{5}$$

We have assumed that the band extends from $-D/2$ to $D/2$ and is symmetric around the origin, i.e.,

$$\int_{-D/2}^{D/2} d\varepsilon\, g(\varepsilon)\varepsilon = 0 \tag{6}$$

for simplicity, z is the number of nearest neighbors to a site, $g(\varepsilon)$ the density of states per site per spin, μ the chemical potential, $n = n_\uparrow + n_\downarrow$ the total site occupation and $m = n_\uparrow - n_\downarrow$ the magnetization per site. We have included an external magnetic field H and use units such that the magnetic moment per electron is unity.

Much of the physics of our model follows from the behavior of I_1, Eq. (5), which is a function of T and m. At infinite temperature, $I_1 = 0$ [from Eq. (6)]. As T is lowered I_1 increases because the states of negative energy (bonding states) become increasingly occupied compared to the ones with positive energy (antibonding states). This causes the prefactor of ε in Eq. (4) to decrease; equivalently, the band narrows, and the density of states and the effective mass increase. When the system starts developing spin polarization I_1 decreases again as more high-energy states become occupied. For full-spin polarization and a half-filled band $I_1 = 0$ again for $T \to 0$ [from Eq. (6)]. By spin polarizing, the system can eliminate the band narrowing effect and achieve as wide a band at $T = 0$ as it possessed at $T = \infty$. In Fig. 1 we illustrate the behavior of I_1 for one case, with a half-filled band and full spin polarization at $T = 0$. The dashed line indicates the values of I_1 below T_c if the system had not spin polarized; for this case, the band would have narrowed to zero width at $T = 0$, where I_1 reaches the value 0.5. In general, I_1 does not reach 0.5 nor does the full line in Fig. 1 reach zero at $T = 0$, but the *qualitative* behavior displayed in Fig. 1 is generic.

The condition that determines the critical temperature is obtained by expanding Eq. (3a) to lowest order in m:

$$1 = \frac{u+j}{1-2jI_1} \int_{-aD/2}^{aD/2} d\varepsilon \frac{g(\varepsilon/a)}{g_0}[-f'(\varepsilon-\mu)] , \tag{7}$$

where g_0 is the density of states at the Fermi energy,

$$u = Ug_0 , \tag{8a}$$

$$j = zJg_0 , \tag{8b}$$

and $a = 1 - 2jI_1$, together with Eqs. (3b) and (5) evaluated at $m = 0$.

Within Stoner theory ($j = 0$), the value of T_c depends crucially on the form of the density of states. For nonconstant density of states and $T_c \ll D$ one can use the Sommerfeld expansion to obtain

$$k_B T_c = \left[\frac{6(u-1)}{\pi^2 u[(g'/g)^2 - g''/g]}\right]^{1/2} \tag{9}$$

with g', g'' the first and second derivatives of the density of states at the Fermi energy. If g is constant throughout the band this obviously fails and T_c is determined by the values of the Fermi function at the bottom and top of the band. For a half-filled band the relation is simply

$$k_B T_c = \left[2 \ln\left[\frac{u+1}{u-1}\right]\right]^{-1} . \tag{10}$$

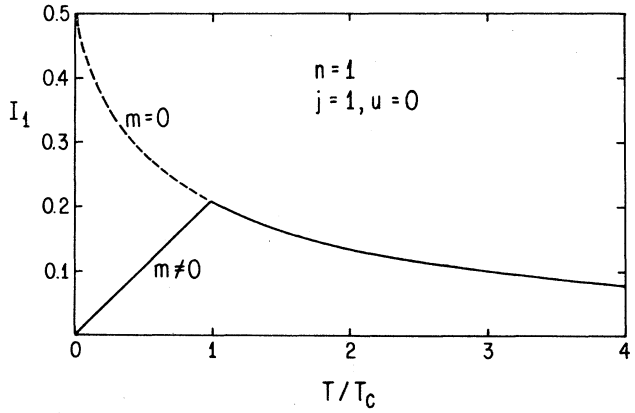

FIG. 1. Behavior of I_1 [Eq. (5)] vs temperature. As T is decreased, I_1 increases until T reaches T_c. Below T_c, I_1 decreases as the system develops spin polarization (solid line). The dashed line shows the behavior of I_1 below T_c if the magnetization is set to zero rather than its self-consistent value.

This strong dependence of T_c on the particular form of the density of states within Stoner theory is disturbing. Since $g(\varepsilon)$ is usually not constant, as sufficiently low temperatures Eq. (9) should be more appropriate. This would imply then that in an alloy system, where the Fermi level can be varied continuously by changing the composition, T_c could undergo wild fluctuations as the Fermi level sweeps through the fine structure in the density of states. Admittedly, some smearing of the fine structure in the density of states will occur in an alloy, but for small compositional disorder one would still except that large changes in T_c would occur from small shifts in the position of the Fermi level. This is not observed, and underscores the serious inadequacy of Eq. (9) to determine the critical temperature.

In our model T_c is determined largely by the behavior of $I_1(T,m)$. Thus we will treat for simplicity the case of constant density of states and assume the temperature is low enough that exponential contributions can be neglected [these effects can easily be included and correction terms of the form (9) and (10) result]. Within these assumptions Eq. (7) is valid also for nonzero m and yields simply

$$1=\frac{u+j}{1-2jI_1(T,m)}\ , \tag{11}$$

which determines the critical temperature from

$$1=\frac{u+j}{1-2jI_1(T_c,0)} \tag{12}$$

and the saturation magnetization at zero temperature m_s from

$$1=\frac{u+j}{1-2jI_1(0,m_s)}\ , \tag{13}$$

as well as the magnetization versus T for $T<T_c$. We recall also that within Stoner theory with constant density of states only a state of full spin polarization is obtained, while Eq. (13) leads naturally to partial spin polarization.

We obtain $I_1(T,m)$ from Eq. (5) by using the Sommerfeld expansion and neglecting exponential contributions as

$$I_1(T,m)=I_1(0,m)-\tfrac{2}{3}\pi^2\left[\frac{k_BT}{D}\right]^2\frac{1}{[1-2jI_1(T,m)]^2}\ . \tag{14}$$

The condition on j to have partial spin polarization is obtained from Eq. (11) setting $T=m=0$:

$$j>j_c=\frac{1-u}{1+2I_1^0} \tag{15}$$

with $I_1^0\equiv I_1(0,0)$. Similarly, to obtain full polarization we need

$$j>\frac{1-u}{1+2I_1(0,n)}\ . \tag{16}$$

The critical temperature is obtained from Eqs. (12), (14), and (15) as

$$\frac{k_BT_c}{D}=\left[\frac{3}{4\pi^2}\right]^{1/2}(u+j)\left[2I_1^0+1-\frac{1-u}{j}\right]^{1/2} \tag{17a}$$

or equivalently

$$\frac{k_BT_c}{D}=\left[\frac{3}{4\pi^2}\right]^{1/2}(u+j)\frac{(2I_1^0+1)^{1/2}}{j^{1/2}}(j-j_c)^{1/2}\ . \tag{17b}$$

For nonconstant density of states Eq. (17) generalizes to

$$\frac{k_BT_c}{D}=\left[\frac{3}{4\pi^2}\right]^{1/2}\times\frac{(u+j)[j(2I_1^0+1)-(1-u)]^{1/2}}{\{[(u+j)/8][(g'/g)^2-g''/g]D^2+jgD\}^{1/2}}\ , \tag{17c}$$

which reduces to Eq. (9) for $j=0$. Note that $j\neq 0$ will substantially smoothen the strong dependence of T_c on density of states predicted by Eq. (9).

For constant density of states $I_1(0,m)$ is easily obtained from Eqs. (3b) and (5):

$$I_1(0,m)=\frac{1-(n-1)^2-m^2}{2}=I_1^0-\frac{m^2}{2} \tag{18}$$

and the saturation magnetization follows from Eqs. (13), (15), and (18) as

$$m_s=\left[\frac{1+2I_1^0}{j}\right]^{1/2}(j-j_c)^{1/2} \tag{19}$$

if the right-hand side is less than n, and $m_s=n$ otherwise. Note that for $m_s\leq n$ critical temperature and saturation magnetization are related by

$$\frac{k_BT_c}{D}=\left[\frac{3}{4\pi^2}\right]^{1/2}[1-2jI_1(T_c)]m_s\ . \tag{20}$$

The magnetization versus temperature is obtained from Eqs. (11) and (14) as

$$m(T)=\frac{2\pi}{\sqrt{3}(u+j)}\frac{k_B}{D}(T_c+T)^{1/2}(T_c-T)^{1/2} \tag{21}$$

if the right-hand side is less than n, and $m(T)=n$ otherwise. Thus we obtain the usual mean-field behavior $(T_c-T)^{1/2}$ close to T_c. Within our approximation this behavior persists away from T_c until the magnetization reaches saturation, and below that temperature $m=n$. This is a somewhat unusual feature, and when exponential corrections are included it is found that $m(T)$ is always smaller than n at finite temperatures. Nevertheless, the qualitative feature of Eq. (21) that the magnetization curve is steeper for a case of full spin polarization compared to one of partial spin polarization is usually correct, as will be seen in the numerical solution in the next section.

The exchange splitting of the bands in our theory is given by

$$\frac{\Delta E}{D}=\frac{(u+j)}{1-2jI_1(0,m_s)}m_s\ . \tag{22}$$

For $m_s \leq n$ we have simply

$$\frac{\Delta E}{D} = m_s \ , \tag{23}$$

and for full polarization

$$\frac{\Delta E}{D} = \frac{u+j}{1-2jI_1(0,n)} n \ . \tag{24}$$

Equations (23) and (20) then yield, for the case of partial polarization, the simple relation

$$\frac{\Delta E}{T_c} = \left[\frac{4\pi^2}{3}\right]^{1/2} \frac{1}{u+j} \ , \tag{25}$$

which in particular is independent of band filling n.

The magnetic susceptibility is obtained from Eq. (3a) by taking the derivative with respect to the magnetic field H and yields

$$\chi(T) = \frac{2\chi_0(T)}{1-(U+Jz)\chi_0(T)} \tag{26}$$

with

$$\chi_0(T) = \int_{-D/2}^{D/2} d\varepsilon \, g(\varepsilon)[-f'((1-2jI_1)\varepsilon - \mu)] \ . \tag{27}$$

Equation (26) has the usual Stoner form, but once again for our case the principal temperature dependence is determined by I_1. For constant $g(\varepsilon)$, and neglecting exponential corrections,

$$\chi_0(T) = \frac{g_0}{1-2jI_1(T,0)} \ , \tag{28}$$

and Eq. (26) becomes, using Eq. (12),

$$\chi(T) = \frac{g_0}{j[I_1(T_c,0) - I_1(T,0)]} \ , \tag{29}$$

which close to T_c gives rise to the Curie-Weiss behavior

$$\chi(T) = \frac{3(u+j)^2}{4\pi^2 g_0 j k_B^2 T_c (T - T_c)} \ . \tag{30}$$

In contrast, for the Stoner case once again the behavior is determined by the density of states. Close to T_c one has (for nonconstant g)

$$\chi(T) = \frac{6g}{\pi^2 u[(g'/g)^2 - g''/g] k_B^2 T_c (T - T_c)} \ , \tag{31}$$

and the effective moment is determined by the fine structure in the density of states, an unphysical result. Both our model and the Stoner model give rise to a Curie-Weiss law close to T_c, but as we will show in the next section, in our case this law is approximately obeyed over a wide temperature range. The physical reason is that even at high temperatures in our model the variation of χ with temperature is enhanced due to the progressive band narrowing. The generalization of Eq. (30) for nonconstant density of states yields

$$\chi(T) = \frac{3(u+j)^2 D}{4\pi^2 \{j + [(u+j)/8](D/g)[(g'/g)^2 - g''/g]\} k_B^2 T_c (T - T_c)} \tag{32}$$

which shows that the effective moment is only weakly dependent on variations in the density of states for $j \neq 0$.

The magnetic energy, including corrections for double counting, is obtained as

$$E = E_0 + \frac{U+Jz}{4} m^2 - \frac{Jz}{2} I_1^2(T,m) \tag{33}$$

with

$$E_0 = \int d\varepsilon \, g(\varepsilon)\{[E_\uparrow(\varepsilon)+\mu] f(E_\uparrow) + [E_\downarrow(\varepsilon)+\mu] f(E_\downarrow)\} \ , \tag{34}$$

and the specific heat is obtained by differentiation. We will discuss its different contributions in limiting cases elsewhere, and here we merely present some numerical results in the next section.

III. NUMERICAL RESULTS

In this section we discuss results obtained by solving the self-consistent equations (3)–(5) for constant density of states. While the analytic results of the previous section are useful to yield qualitative insight, at finite temperatures exponential corrections do play a varying role that depends on the temperature, and it is preferable to include them by solving the equations numerically to avoid altering the systematics. The correction terms are proportional to exponentials of $(-nD/k_BT)$ and $(n-2)D/k_BT$ and are negligible in the weak ferromagnetic regime. We will use units of D/k_B for the temperature.

We will not attempt a microscopic determination of our interaction parameters U and J for any particular case. As discussed in I, the role of U in our equations is surely grossly overestimated by the mean-field decoupling procedure. Instead, we regard u and j as phenomenological parameters, with $(u+j)$ giving rise to the exchange splitting and j giving rise to the band narrowing. It is even possible that u should be taken close to zero when the effect of correlations is taken into account. We recall from I that the values of the parameters to give rise to magnetization varying from weak to strong is

$$\frac{1}{2} \leq \frac{j}{1-u} \leq 1 \ , \tag{35}$$

which even for $u = 0$ is not an unreasonable range for the two-center exchange integral $J = j/zg_0$, Eq. (2).

Figure 2 shows the behavior of the saturation magnetization m_s as a function of band occupation. As discussed

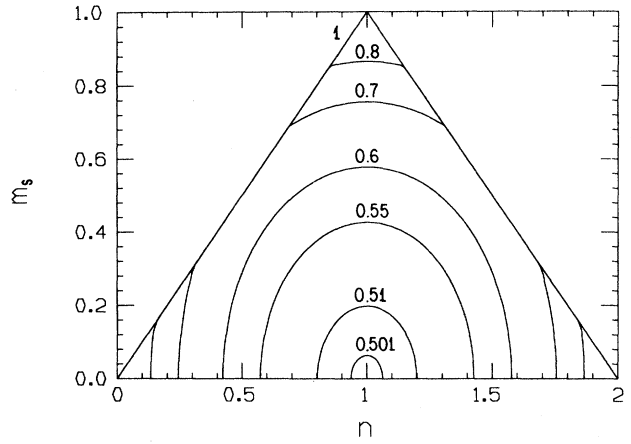

FIG. 2. Saturation magnetization m_s [Eq. (19)] vs band filling for various values of $j/(1-u)$ (numbers next to curves).

in I, the curves for $j/(1-u)\sim 0.7$ or 0.8 resemble the behavior found in the $3d$ transition-metals series encompassing Fe, Co, and Ni. Weak ferromagnetism (small saturation magnetization) is most easily obtained close to the half-filled band, with $j/(1-u)$ approaching 0.5. For other fillings weak ferromagnetism is also possible but the parameter range narrows rapidly as one moves away from $\frac{1}{2}$ filling, as shown in Fig. 3 of I.

Figure 3 shows the behavior of the critical temperature versus occupation. It follows approximately the behavior of the saturation magnetization, as expected from Eq. (20). The ratio of T_c/m_s is accurately given by Eq. (20) for the case $j=0.51$ ($T_c/m_s=0.141$) and approximately for the other cases, the ratio being somewhat smaller than predicted by Eq. (20): for $j=0.6$, $T_c/m_s\sim 0.14$ to 0.15 while Eq. (20) gives 0.165, and for $j=0.8$, $T_c/m_s\sim 0.18$ to 0.21, while Eq. (20) gives 0.221.

While the saturation magnetization depends only on the ratio $j/(1-u)$, T_c has a weak additional dependence on u. From Eq. (17) we obtain, for fixed $\bar{j}=j/(1-u)$:

$$\frac{T_c(u=u_1)}{T_c(u=u_2)}=\frac{1+u_1(1/\bar{j}-1)}{1+u_2(1/\bar{j}-1)} \tag{36}$$

so that T_c should increase with increasing u if $j/(1-u)$ is kept constant, the effect being larger the smaller $\bar{j}$. We find the relation (36) to be accurately satisfied for $j=0.51$, for the larger j's the deviations are towards smaller T_c's for increasing u than predicted by Eq. (36). In fact, T_c can also decrease for increasing u. Figure 4 shows the behavior for $n=1$. The behavior for other values of n is similar, with the decreasing behavior of T_c with u setting in at smaller u as n moves away from $n=1$.

Figures 3 and 4 illustrate that the values of T_c are strongly determined in our model and cannot be changed without also changing the saturation magnetization or the filling. With nonconstant density of states we believe it would be possible to alter the behavior somewhat, in particular allowing T_c to increase when n is moving away from 1 in Fig. 3. This would be necessary to explain the larger critical temperature in Co as compared to Fe. The bandwidth of the e_g states in the $3d$ ferromagnetic transition metals is approximately 2 eV. For $j=0.8$ our theory then would predict (assuming $n=1$) a T_c between 2000 and 3700 K depending on the value of u, which is larger than the experimental value for Fe but a factor of 2 smaller than what has been obtained from the local spin-density functional formalism.[14] Incorporating the detailed band structure in our model may result in accurate values for T_c.

We consider next the behavior of the magnetic susceptibility above T_c. Approximate Curie-Weiss behavior is found for a wide range of parameters. We parametrize the susceptibility as

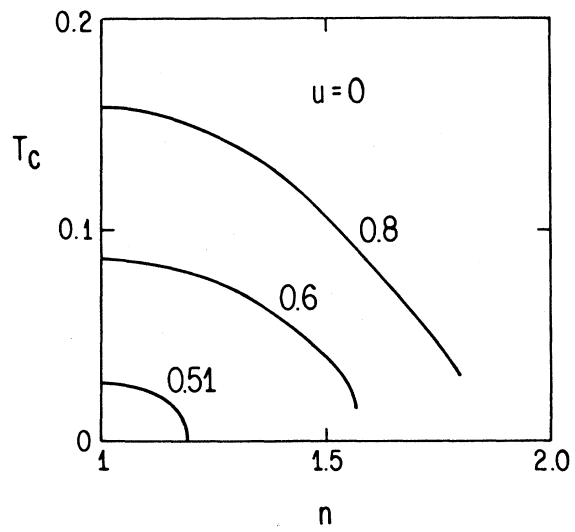

FIG. 3. Critical temperature (in units of D/k_B) vs occupation for three values of j (numbers next to the curves) for $u=0$.

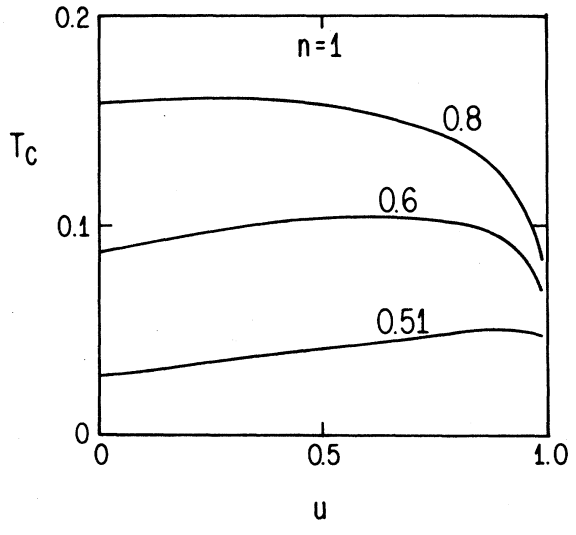

FIG. 4. Critical temperature (in units of D/k_B) vs u for band filling $n=1$ and various value of j (numbers next to the curves).

$$\chi(T)=\frac{p_{\rm eff}^2(T)}{3(T-T_c)}\ , \tag{37}$$

and study the behavior of the effective moment $p_{\rm eff}$. Figure 5 shows its temperature dependence for $j=0.8$, $u=0$, and four values of the density. We show a temperature range up to eight times the critical temperature, the same smooth behavior persists at higher temperatures. The nearly temperature independence of the effective moment is striking, particularly at the higher densities. The effective moment at infinite temperature is given by

$$p_{\rm eff}(T=\infty)=\left[3n\left[1-\frac{n}{2}\right]\right]^{1/2}\ . \tag{38}$$

At $T=T_c$, the effective moment in Fig. 5 is larger than at $T=\infty$ by only 3.2%, 3.4%, 4.8%, and 13% for $n=1$, 0.75, 0.5, and 0.25, respectively.

Figure 6 shows the variation in the temperature dependence as j is lowered, for fixed n ($n=1$). The effective moment becomes slowly more temperature dependent as j decreases, but it is only for very weak ferromagnetism that the temperature dependence becomes appreciable. Surprisingly, the effective moment becomes *larger* as j decreases, opposite to what a localized picture of magnetism would predict. This can be understood from Eq. (30), as the dominant change as j decreases is the reduction in T_c. The same trend is observed for other values of n.

Figures 7 to 9 show the effect of u on the behavior of the effective moment. We chose the values of u and j so as to keep the critical temperature constant in each case. The temperature dependence of $p_{\rm eff}$ increases as u increases but is still small for $u\sim 0.5$. In the Stoner limit $j=0$, the temperature dependence becomes substantial, particularly for smaller critical temperatures. The same qualitative trends are found for other cases, both for parameters giving rise to full and partial spin polarization.

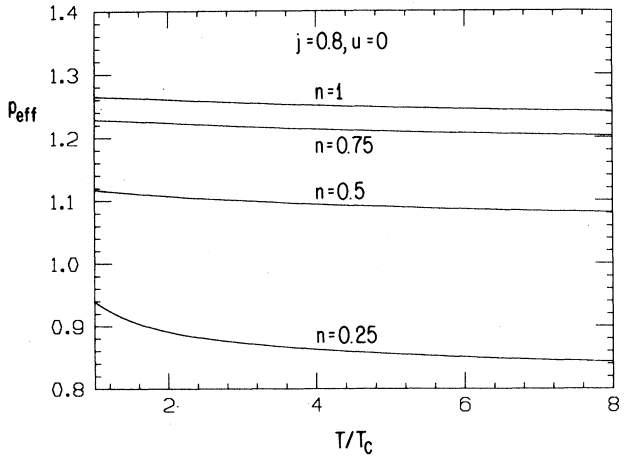

FIG. 5. Effective Curie-Weiss moment $p_{\rm eff}$ defined by Eq. (35) vs temperature for various values of the density. $T_c=0.158$, 0.145, 0.107, and 0.044 for $n=1$, 0.75, 0.5, and 0.25, respectively. The saturation magnetization is $m_s=0.866$ for $n=1$ and $m_s=n$ for the other n values.

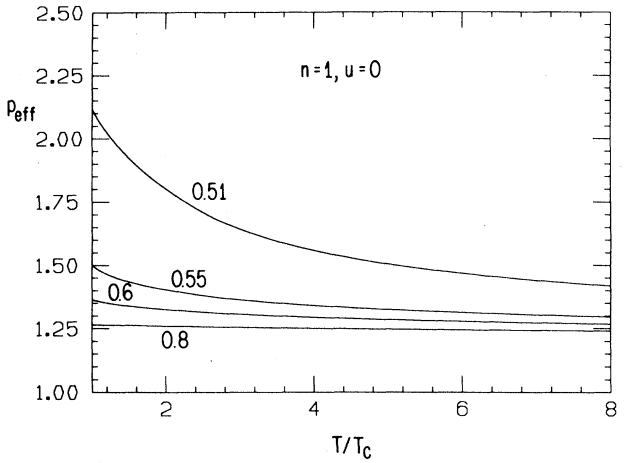

FIG. 6. Effective moment vs temperature for various values of j (numbers next to the curves) for $n=1$, $u=0$. $T_c=0.158$, 0.0863, 0.0612, and 0.0278, and $m_s=0.866$, 0.577, 0.426, and 0.198 for $j=0.8$, 0.6, 0.55, and 0.51, respectively.

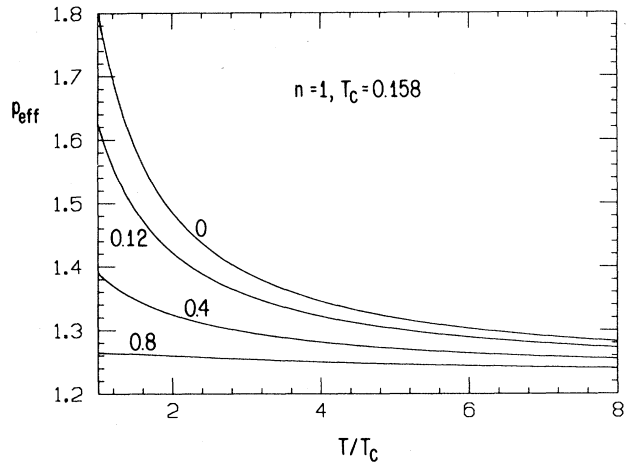

FIG. 7. Effective moment vs temperature for band filling $n=1$ and various values of j and u chosen so that the critical temperature remains fixed at $T_c=0.158$. The values of j are given next to the curves, and $u=0$, 0.5, 0.9, and 1.088 for $j=0.8$, 0.4, 0.12, and 0, respectively.

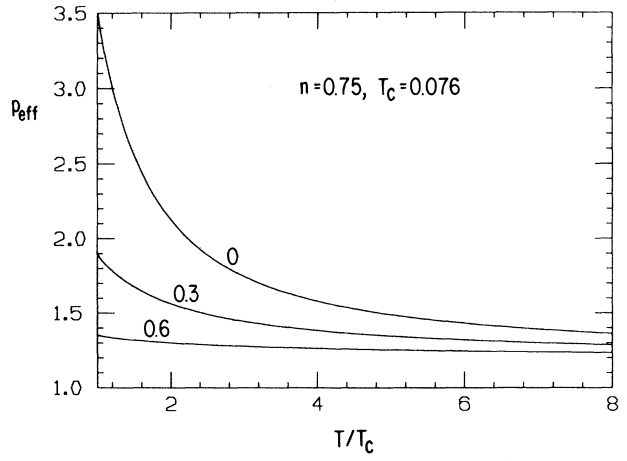

FIG. 8. Same as Fig. 7 for $n=0.75$, $T_c=0.076$. $u=0$, 0.5, and 1.007 for $j=0.6$, 0.3, and 0, respectively.

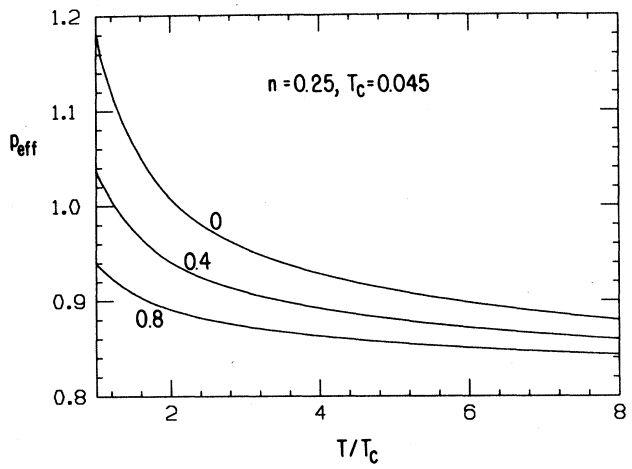

FIG. 9. Same as Fig. 7 for $n=0.25$, $T_c=0.0045$. $u=0$, 0.5, and 1.064 for $j=0.8$, 0.4, and 0, respectively.

The factors that determine the temperature dependence of p_{eff} are principally the magnitudes of u and of the critical temperature.

We next consider the behavior of the magnetization versus temperature below T_c. Figure 10 shows $m(T)$ for $j=0.8$ and three values of the density. The magnetization curve becomes steeper as n decreases because the system is more strongly ferromagnetic; this is in accordance with our finding in the previous section, and consistent with the behavior found in transition metals. The effect of a nonzero u, adjusting j to yield the same critical temperature, is to make the magnetization curve somewhat less steep, as shown in Fig. 11. It is well known that Stoner theory tends to yield magnetization curves that are not steep enough compared to experimental findings.[8]

A good indicator of the steepness of the magnetization curve is the value of $m(T)$ at $T=T_c/2$. In Figs. 12 and 13 we plot

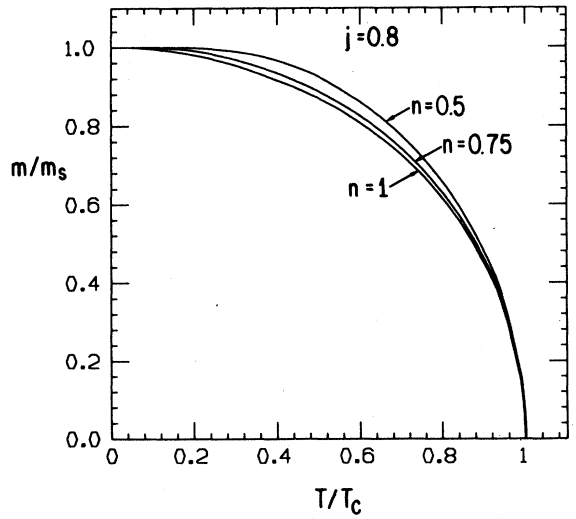

FIG. 10. Reduced magnetization vs temperature for $u=0$, $j=0.8$ and three values of the density. $m_s=0.866$, 0.75, and 0.5 for $n=1$, 0.75, and 0.5, respectively.

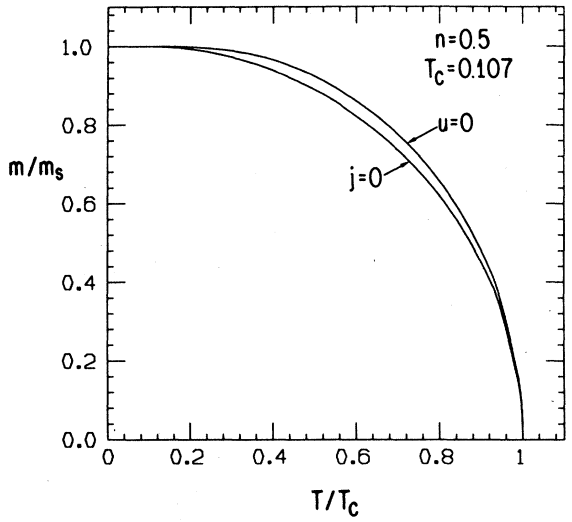

FIG. 11. Reduced magnetization vs temperature for $n=0.5$ and $T_c=0.107$. The case with $u=0$ has $j=0.8$, and the one with $j=0$ has $u=1.108$. $m_s=n$ in both cases.

$$m_{1/2}\equiv m(T=T_c/2)/m(T=0) \tag{39}$$

versus j for $n=1$ and $n=0.5$, together with the saturation magnetization m_s. $m_{1/2}$ attains its minimum value at the value of j where the system becomes fully magnetized, $m_s=n$. This minimum value is smaller the smaller n is, and the overall variation of $m_{1/2}$ increases as n decreases. As $T\to 0$, using Eqs. (20) and (21) we obtain

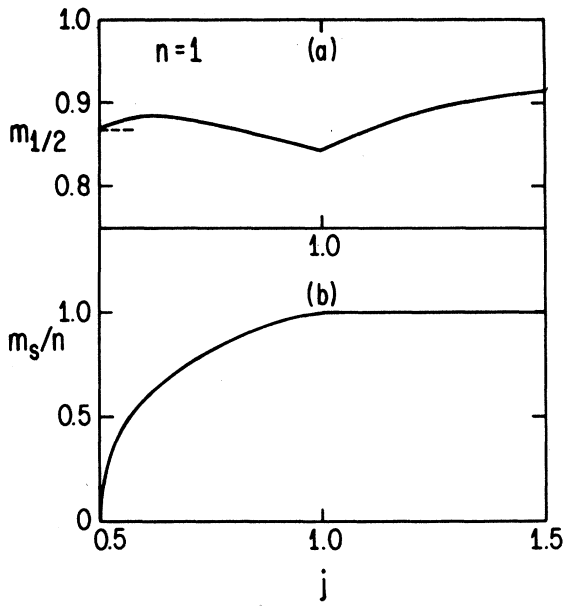

FIG. 12. (a) Reduced magnetization at $T/T_c=0.5$ [Eq. (37)] vs j, and (b) saturation magnetization vs j for $n=1$, $u=0$. Note that the minimum in $m_{1/2}$ coincides with the point where full saturation magnetization is reached, and that as j is reduced $m_{1/2}$ approaches the limiting value given by Eq. (40) (dashed line).

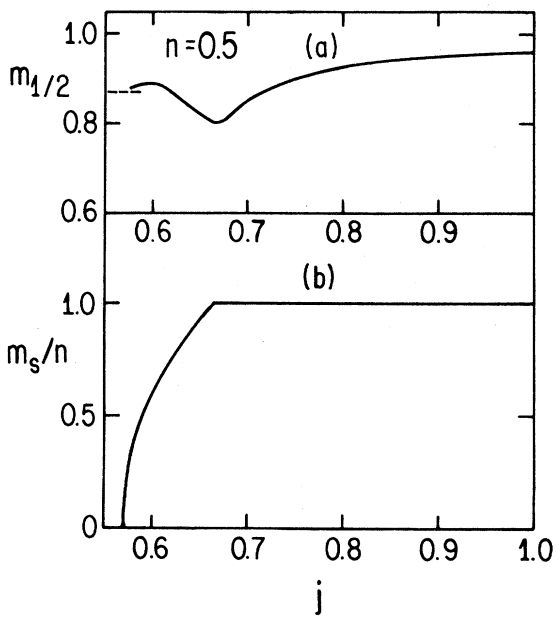

FIG. 13. Same as Fig. 12 for $n=0.5$.

$$\frac{m(T)}{m(0)}=\left[1-\left[\frac{T}{T_c}\right]^2\right]^{1/2} \tag{40}$$

which yields $m_{1/2}=0.866$, and is indicated by the dashed lines in Figs. 12 and 13. It will be interesting to correlate these results with observations in ferromagnetic metals and alloys.

Finally, we show two examples of specific heat versus temperature obtained from differentiation of Eq. (33) in Figs. 14 and 15. As before, we choose parameters to keep T_c fixed and examine the cases $u=0$ and $j=0$. The most striking effect of j is to make the specific-heat jump at T_c larger, by approximately a factor of 2. This occurs because of the additional contribution resulting from the change in slope of I_1 at T_c (Fig. 1). Too small specific-heat jumps have been a serious drawback of Stoner theory, and the order of magnitude of the increase shown in Figs. 14 and 15 for $j\neq 0$ is what is approximately needed to obtain agreement with experimental observations.

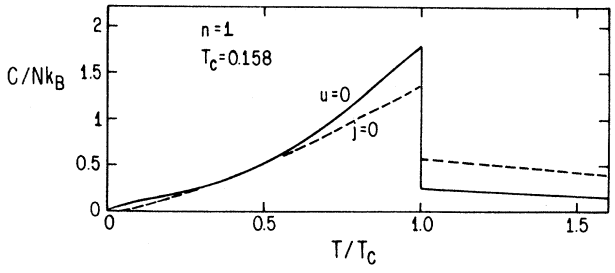

FIG. 14. Specific heat vs temperature for $n=1$ and values of u and j chosen, so that the critical temperature remains fixed at $T_c=0.158$. $j=0.8$ for $u=0$ (solid line) and $u=1.088$ for $j=0$ (dashed line).

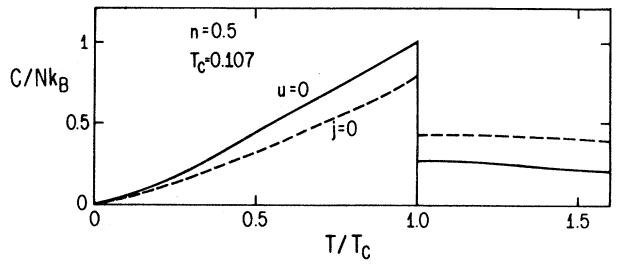

FIG. 15. Specific heat vs temperature for $n=0.5$, $T_c=0.107$. $j=0.8$ for $u=0$ (solid line) and $u=1.108$ for $j=0$ (dashed line).

IV. SUMMARY AND DISCUSSION

We have explored finite-temperature properties of a new model proposed to describe metallic ferromagnetism.[1] The interaction responsible for ferromagnetism in this model is a Coulomb matrix element J that lowers the energy when electrons of opposite spin at the Fermi surface are in states of opposite bonding character. Thus, the optimal case for ferromagnetism for given parameters occurs for the half-filled band case and for structures that can accommodate purely antibonding states without frustration, like bcc. As discussed in Sec. II, the physics that drives ferromagnetism in our model is the band narrowing caused by the interaction J as the temperature is lowered, which leads to spin polarization as a way to suppress the band narrowing effect.

For fixed interaction parameters our model leads to a dependence of saturation magnetization on band filling that is consistent with the Slater-Pauling curve.[9] In Fig. 2, iron would fall near $n=1$, Co around $n=1.3$, and Ni around 1.7, with $j/(1-u)$ around 0.8. Actually, it is likely that the parameters do change somewhat with filling, with j probably becoming larger as the filling increases. This would still lead to full spin polarization in our model for Co and Ni but possibly account for the higher critical temperature in Co as compared to Fe, while still lead to lower T_c for Ni as indicated by Fig. 3. Additionally, variations in the density of states will cause some variations on top of the ones found in our model for constant density of states.

The magnetic susceptibility above T_c was found to accurately follow Curie-Weiss behavior, consistent with experimental observations. The Curie-Weiss behavior is one of the properties that have tended to favor localized models of magnetism over band models. However, localized models cannot possibly account for the large Curie-Weiss moment found in ferromagnets with very small saturation magnetization, while our theory naturally predicts such behavior, as shown in the previous section. The specific heat jump at T_c was found to be considerably increased in our model and of the right order of magnitude to resolve the discrepancy of the Stoner model prediction with experimental observations.[10]

The behavior of magnetization versus temperature below T_c was found to be steeper than that obtained from Stoner theory, and to show trends consistent with obser-

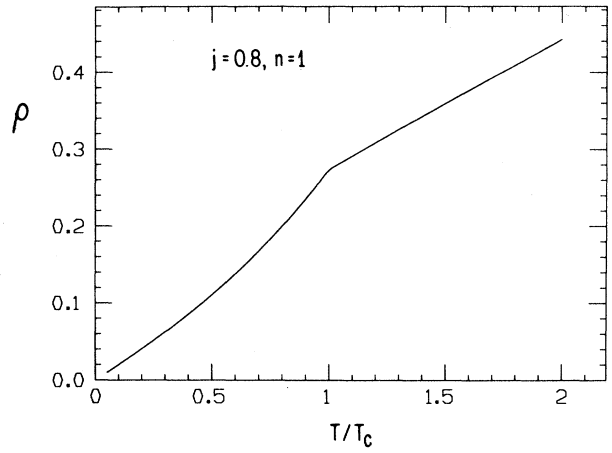

FIG. 16. Typical behavior for resistivity from our model. The form Eq. (41) for ρ is plotted, with τ linear in temperature and m^* given by Eq. (42). The vertical scale units are arbitrary. $u=0$.

vations. Our model can easily yield magnetization curves steep enough to account for the observed ones in Ni, while this is not possible with the Stoner model.[10] For example, for $n=0.3$ and $j=0.9$ we find $m_{1/2}=0.94$, consistent with the value for Ni. For this case, $T_c/D=0.078$.

The anomalous drop in resistivity below the Curie temperature is naturally explained by our model due to the band broadening that occurs as spin polarization develops. Consider the simple Drude formula for electrical resistivity

$$\rho=\frac{m^*}{ne^2\tau} \tag{41}$$

and assume a linear dependence of relaxation time τ on temperature due to phonon scattering for simplicity (strictly speaking, only valid well above the Debye temperature). A temperature dependence in the effective mass m^* will arise from the prefactor of ε in Eq. (4), given by

$$m^*(T)=\frac{m^*(\infty)}{1-2jI_1(T,m)} . \tag{42}$$

The temperature dependence of $I_1(T,m)$ discussed in Sec. II leads to a typical behavior of the resistivity Eq. (41) as shown in Fig. 16 for one case. The break displayed at T_c resembles the behavior found in ferromagnetic metals,[13] and its origin becomes transparent in our model. Alternative explanations of this effect have invoked reduced spin-flip scattering as the system orders magnetically.[15]

Our model naturally leads to except anomalous thermal expansion behavior below T_c. As the driving force for ferromagnetism is occupation of antibonding states by majority spins and reduced occupation of bonding states by minority spins, this will lead to a tendency for the lattice to expand as spin polarization develops, which will counter the normal contraction tendency due to reduced lattice vibrations as the temperature is lowered. The competition of these two tendencies can then lead to the Invar effect, i.e., zero coefficient of thermal expansion. The fact that the anomalously large lattice constants in ferromagnetic metals is due to increased occupation of antibonding states was pointed out by Janak and Williams,[16] and fits naturally in our model. Other thermal properties of this model, as well as detailed comparison with observations in ferromagnetic metals and alloys, will be reported in forthcoming papers.

An important consequence of our model is that it naturally leads to the prediction that hydrogen in the metallic state should exhibit weak ferromagnetism.[17,1] This is contrary to the commonly held view that metallic hydrogen should be a high temperature superconductor,[18] and should have wide astrophysical implications.

ACKNOWLEDGMENTS

This work was supporrted by the University of California, San Diego, La Jolla, CA 92093.

[1] J. E. Hirsch, Phys. Rev. B **40**, 2354 (1989).
[2] J. Hubbard, Proc. R. Soc. London, Ser. A **276**, 238 (1963).
[3] *Magnetism of Metals and Alloys,* edited by M. Cyrot (North-Holland, Amsterdam, 1982).
[4] *Ferromagnetic Materials,* edited by E. P. Wolfarth (North-Holland, Amsterdam, 1980).
[5] *Electron Correlation and Magnetism in Narrow Band Systems,* edited by T. Moriya (Springer, Berlin, 1981), p. 2.
[6] M. B. Stearns, Phys. Today **31**, 34 (1978).
[7] See various contributions in Ref. 5, particularly by T. Moriya, R. E. Prange, H. Hasegawa, and J. Hubbard.
[8] E. P. Wolfarth, in Ref. 4, p. 1, and references therein.
[9] F. Gautier, in Ref. 3, p. 1, and references therein.
[10] E. P. Wolfarth, Philos. Mag. **42**, 374 (1951).
[11] E. C. Stoner, Proc. R. Soc. London, Ser. A **165**, 372 (1938).
[12] M. A. Shimizu, A. Katsuki, and H. Yamado, J. Phys. Soc. Jpn. **20**, 396 (1965).
[13] J. M. Ziman, *Electrons and Phonons* (Oxford University, Oxford, 1960), p. 380.
[14] O. Gunnarson, Physica B **91**, 329 (1977).
[15] P. G. de Gennes and J. Friedel, J. Phys. Chem. Solids **4**, 71 (1958).
[16] J. F. Janak and A. R. Williams, Phys. Rev. B **14**, 4199 (1976).
[17] J. E. Hirsch, Phys. Lett. A (to be published).
[18] N. W. Ashcroft, Phys. Rev. Lett. **21**, 1748 (1968); T. W. Barbec III, A. Garcia, and M. L. Cohen, Nature **340**, 369 (1984).